Impact of Rainfall on the Retrieval of Soil Moisture using AMSR-E data

Kyoung-Wook Jin, Eni Njoku, Steven Chan
Jet Propulsion Laboratory, California Institute of Technology
4800 Oak Grove Drive, Pasadena, CA 91109 USA
kwjin@jpl.nasa.gov

Abstract—Rainfall leads to errors and limitations on the soil moisture retrieval using satellite radiometry. To understand the impact of rainfall, we examined the temporal and spatial correlations between rainfall and soil moisture using AMSR-E (Advanced Microwave Scanning Radiometer-EOS) data. Scan by scan (swath basis) analyses were conducted to find the short time scale relationship between the two physical parameters. The retention of soil moisture after rainfall in different climatic regimes (e.g. humid and arid regions) was also examined.

Keywords-precipitation; rainfall; soil moisture; remote sensing; microwave; AMSR-E

I. INTRODUCTION

Retrieval of soil moisture using satellite data is important for better understanding of the global water cycle and its role in climate change. In addition, rainfall measurement over land is a crucial element in understanding the water cycle exchange between land and atmosphere. Precipitation is highly related with soil moisture. However, it is very difficult to study the direct relationship between the two variables since precipitation is a main source of uncertainty in soil moisture retrieval. In general, retrieval of soil moisture is not attempted in the presence of precipitation due to the complexity of discerning the signal emitted by the surface from that of a raining atmosphere.

The AMSR-E (Advanced Microwave Scanning Radiometer-EOS) instrument on the Aqua satellite launched on May 4, 2002, provides an improved opportunity for soil moisture retrieval study due to its multiple channels (e.g. 6.925, 10.65 and 18.7GHz with dual polarizations) and enhanced resolutions with respect to previous sensors. With AMSR-E data, two retrieved physical parameters (rainfall and soil moisture) can be utilized simultaneously. In this study, we focused on the temporal and spatial relationship between precipitation and soil moisture from AMSR-E data.

II. METHODS

A. Soil Moisture Algorithm

Passive microwave techniques to retrieve near-surface soil moisture have been developed from the theoretical basis which relates the emitted microwave radiation from land surface to the dielectric properties of sub-surface soil moisture. Njoku and Kong [1] presented the theory of passive microwave remote sensing of soil moisture. However, developing a retrieval algorithm based on a satellite observation is very difficult due to the many sources of uncertainties. Furthermore, to achieve robust brightness temperature sensitivity to the surface moisture content, low frequency channels (1-3GHz) are highly preferable through vegetation and their deeper penetration depth. However, Njoku et al. [2] have shown that promising results are feasible using the AMSR-E (Advanced Microwave Scanning Radiometer-EOS) for soil moisture retrieval.

In this study, we used an updated version of the AMSR-E soil algorithm [2]. This algorithm utilizes the polarization ratio (pr10) at 10GHz (~ 3cm wavelength) which is defined as

$$pr10 = (Tb10v - Tb10h) / (Tb10v + Tb10h),$$

where Tb10v and Tb10h are the brightness temperatures of the vertically and horizontally polarized AMSR-E channels respectively.

The variations of pr10 with respect to the monthly minimum polarization ratio of the 10GHz are interpreted as the short-term dynamic soil moisture signal. The algorithm has some limitations. For example, the use of single channel (10GHz) results in a very shallow sensing depth (~1cm). The longer wavelength 6.9 GHz data were not used due to the contamination at this frequency in many regions by Radio Frequency Interference [3]. In addition, the soil moisture estimation over dense vegetation areas leads to greater errors.

B. Land Rainfall Algorithm

For land rainfall algorithm, an empirically-based algorithm has been developed ([4], [5]), that utilizes the depression of the brightness temperatures at high-frequencies (e.g. 85 GHz) due to the scattering by ice particles aloft. The current operational rainfall algorithm (NASA, level 2 rainfall algorithm, GPROF, for SSM/I, TMI and AMSR-E) has adopted this concept for precipitation over land. Like soil moisture estimation, retrieval of precipitation has many uncertainty sources such as the high variability of the ice particle size distribution, false rain signatures caused by snow cover, deserts, and semiarid land plus the uncertainty of rain type classification.

C. Data

For comparison with the swath basis AMSR-E level 2 rain products [6], we retrieved surface soil moisture on a pixel-by-pixel (or swath) basis using AMSR-E Level 2A brightness temperature data [7]. For analysis of daily level 3 products, the official AMSR-E Level 3 surface soil moisture data [8]

were directly used. In addition to the AMSR-E rainfall products, two independent precipitation data sets are included: GPCP (Global Precipitation Climatology Project) 1-Degree Daily Combination data and Rain Gauge data from NCDC (National Climatic Data Center).

III. RESULTS

Our study is an ongoing project and more detailed results will be presented in the future based on our further investigations. In this paper we provide only preliminary results based on limited analyses.

A. Swath Basis Analysis

To remove the possible rain-contaminated pixels, a screening method [9] is implemented. However, the current GPROF algorithm uses slightly changed threshold values for AMSR-E channels (Tb24v-Tb89v > 8K, and Tb89v < 270K). First, to evaluate the effectiveness of this method, two granules are selected, one over Africa (10-30N; 0-20E) and another over the U.S. (85-105W; 30-48N).

The rain flag map is plotted over the both regions (Figs. 1(a) and 2(a)). The color of each pixel indicates the difference between the two channels, i.e., Tb24v-Tb89v. The black color denotes the raining pixels with rain as estimated by the rain-flag screening. For comparison, level 2 rain rates retrieved from GPROF algorithm are plotted in Figs. 1(b) and 2(b).

Compared to the areas of screened raining pixels, the retrieved raining areas are smaller. It could thus be assumed that the screening thresholds are very conservative. Another possibility is that the retrieved rainfall areas (from GPROF) are narrower than actual raining areas. The NEXRAD national mosaic radar reflectivity image (Fig. 3(a), from www4.ncdc.noaa.gov) shows that possible raining areas are much wider with respect to the satellite observation. The AMSR-E measurement (vertically polarized 89GHz channel) corresponding in terms of time and space to Fig. 3(a) is presented in Fig. 3(b).

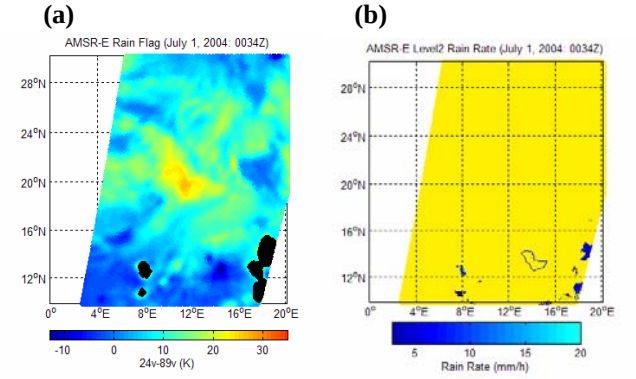

Figure 1. (a) Rain flag for a pass of AMSR-E over the Africa (10-30N; 0-20E). The data span approximately 5 minutes, (b) AMSR-E level 2 rain rate corresponding to (a). The black color in Figure 1(a) represents pixels with rain.

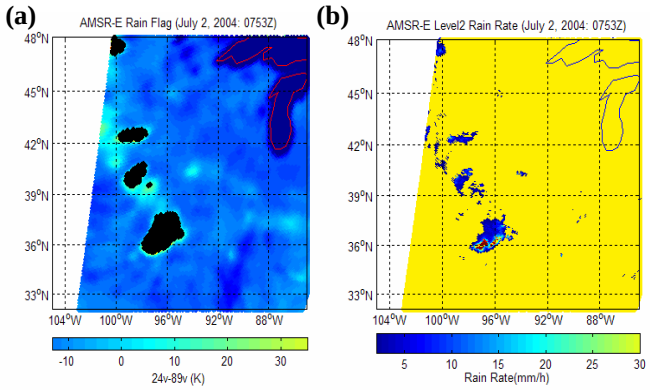

Figure 2. (a) Rain flag for a pass of AMSR-E over the United States (32-48N; 85-105W). The data span approximately 4 minutes, (b) AMSR-E level 2 rain rate corresponding to (a). The black color in Figure 2(a) represents raining pixels.

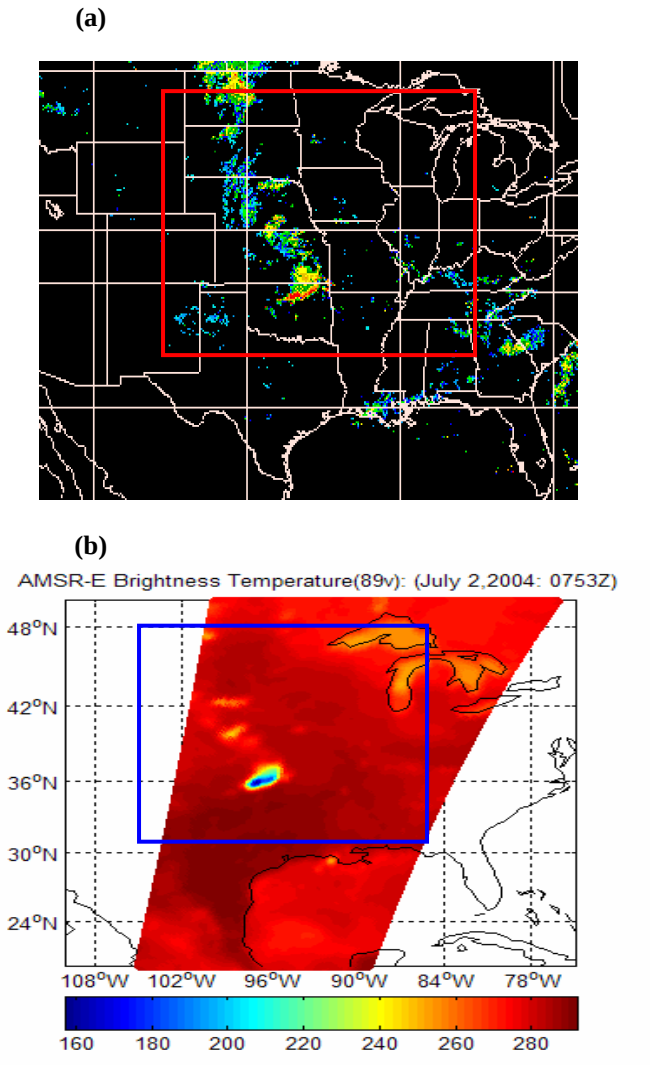

Figure 3. (a) The NEXRAD national mosaic reflectivity image from NCDC (July 2, 2004: 0800Z), (b) Tb89v channels of AMSR-E over the United States (July 2, 2004: 0753Z). The data span approximately 8 minutes and thus the observation period between (a) and (b) is very close each other.

To investigate further, a plot of Tb89v as a function of the Tb24v-Tb89v was generated using all samples over the selected region shown in Fig. 1. Screened raining pixels are indicated by blue. It is clear that most samples, at which the brightness temperatures of the 89v are greater than about 275K, are non-raining pixels. But, it is found that screening of raining pixels is heavily driven by the one threshold (Tb89v < 270K) rather than the combined effect (Tb24v-Tb89v > 8K and Tb89v < 270K).

Second, we examined the impact of rainfall on the retrieval of soil moisture for the same data shown in Figs. 1 and 2. The data are highlighted by the blue box in Figs. 5 and 6 which show the retrieved soil moisture over Africa and the United States. In this analysis, the rain screening process was not applied. As a result, the retrieved values over some areas (e.g. west-central Africa) are rain-contaminated.

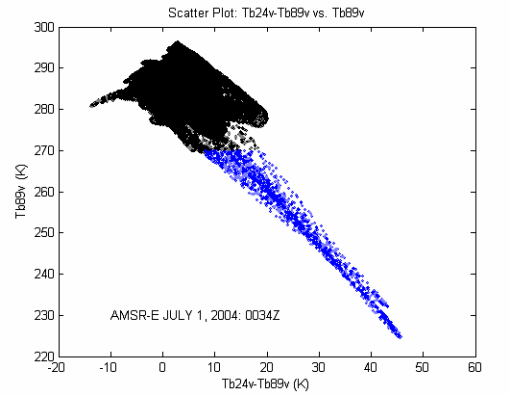

Figure 4. Relationship between the 89GHz vertically polarized brightness temperature and the rain flag (Tb24v-Tb89v) for the data shown in Figure 1. Blue represents the raining pixels

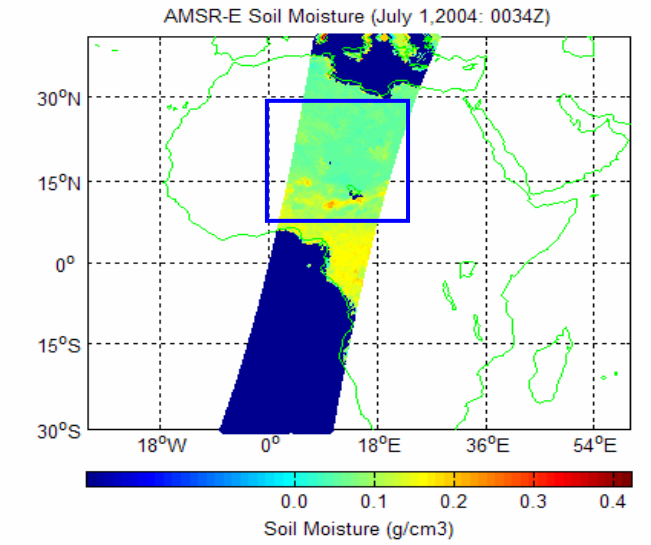

Figure 5. Retrieved soil moisture over Africa from the selected granule (AMSR-E, July 1, 2004: 0034Z), Note that the retrieved values over some area are not meaningful (e.g. mountainous area and over the ocean) because proper land mask schemes are not implemented in this analysis.

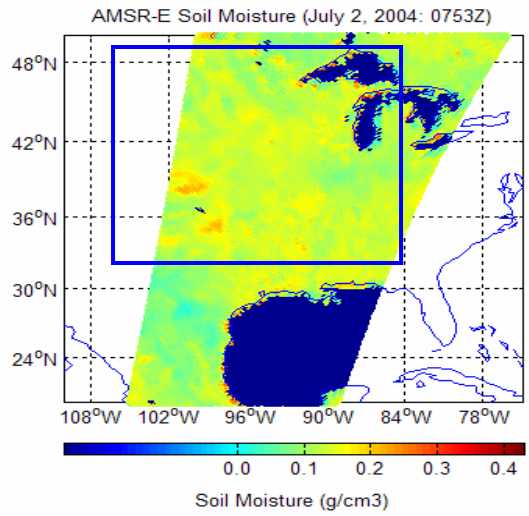

Figure 6. Retrieved soil moisture over the United States from the selected granule (AMSR-E, July 2, 2004: 0753Z)

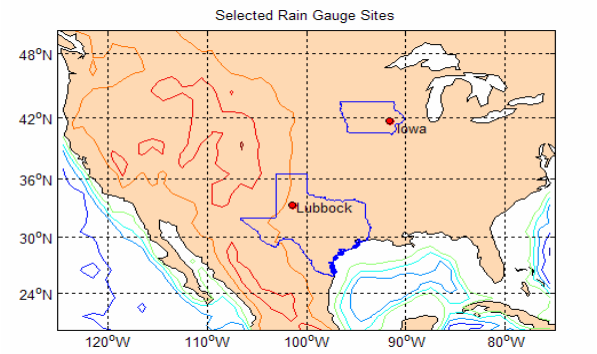

Figure 7. The selected two rain gauge sites for the time series analysis: Iowa City, Iowa (41.72N91.66W) and Lubbock, Texas (33.39N; 101.49W)

The soil moisture over raining areas clearly shows the impact of rainfall. While many areas are contaminated by false signals due to the rainfall, some areas that surround raining cores show effects of the increased moisture due to the precipitation. They also indicate that the change of soil moisture highly relies on the intensity and duration of rainfall driven by the two different rainfall regimes (e.g. convective and stratiform rain). However, clear understanding of the rainfall impact on soil moisture in this scale requires a solid rain screening method along with a finer resolution of observation.

B. Time Series Analysis

Fig. 7 shows two selected rain gauge sites for analysis: Iowa City, Iowa (latitude 41.72N, longitude 91.66W) and Lubbock, Texas (latitude 33.39N, longitude 101.52W). We assumed that Iowa represents a wet area and Lubbock for a dry area. The soil moisture variation as a function of time (July, 2004) is plotted in Figs. 8(a) and 9(a). Two independent rainfall data sets were compared with the retrieved soil moisture (Figs. 8(b) and 9(b)). One data set consists of rain

gauge data and the other consists of GPCP rain data. For the comparison, closest points with respect to the rain gauge sites were selected from both GPCP rain data (1° x 1° grid format) and the AMSR-E daily soil moisture products (25km x 25km EASE-Grid format).

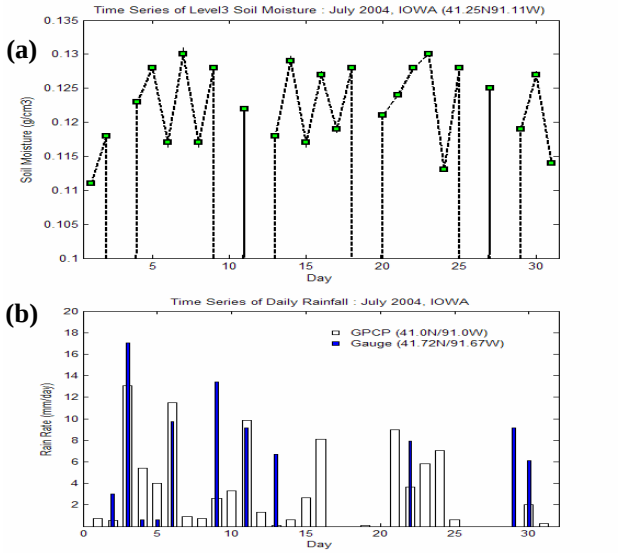

Figure 8. (a) Retrieved daily soil moisture as a function of time (July 2004, Iowa), (b) GPCP(white) and Rain Gauge (blue) rainfall (mm/day) corresponding to a).

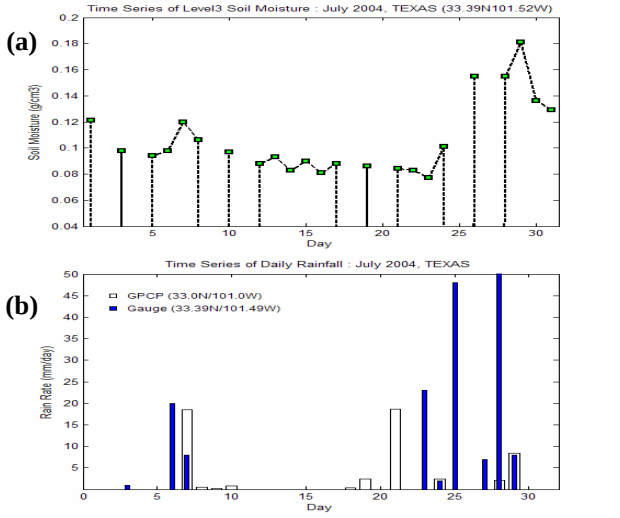

Figure 9. (a) Retrieved daily soil moisture as a function of time (July 2004, Texas), (b) GPCP(white) and Rain Gauge (blue) rainfall (mm/day) corresponding to a).

Direct comparison between point measurements (rain gauge) and spatially averaged snapshots (satellite measurements) leads to a large discrepancy. Due to the location mismatch, rainfall data from rain gauges in Fig. 8(b) show much smaller raining events compared to GPCP data, which are satellite data combined with rain gauge data. Some days (e.g. July 3 and 9) show that gauge data have a larger daily rain rates than GPCP. In the Fig. 9(b), the discrepancy between the two data sets is obvious as well.

Nonetheless, the figures give us some insights into the relationship between rainfall and soil moisture. It is found that retrieved soil moisture does vary according to the major rainfall events. At the Iowa site (wet region), the soil moisture variation is relatively small (0.11 ~ 0.13g/cm3) and the response to the rainfall is not as sensitive. In the case of the Texas site (dry region), the significant change of soil moisture is clearly observed just after the heavy rainfall events (July 25 and 29). However, to determine better the relationship between the two variables (Gauge data vs. Satellite data), more sampled data sets which are co-registered in terms of space and time are required.

CONCLUTIONS

The preliminary results give us some insights into the relationship between precipitation and soil moisture. For better understanding of the rainfall impact on soil moisture retrieval, many limitations of the current soil moisture and land rainfall algorithms need to be resolved as well as further comparative analyses done. In particular, the current rain screening method requires improvements by providing a more effective scheme to discern the intensity and spatial distribution of rainfall.

ACKNOWLEGMENT

This work represents one phase of research carried out at the Jet Propulsion Laboratory (JPL), California Institute of Technology, under contract with the National Aeronautics and Space Administration. Kyoung-Wook Jin is currently in the NASA Postdoctoral Program at JPL.

REFERENCES

[1] E.G. Njoku and J.A. Kong, “Theory for passive microwave remote sensing of near-surface soil moisture,” *J. Geophys.Res.*, vol. 82, 3108-3118, 1977.

[2] E.G. Njoku, T.J. Jackson, V.,Lakshmi, T.K.Chan, S.V.Nghiem, “Soil moisture retrieval from AMSR-E,” *IEEE Trans. Geosci. Remote Sensing*, vol. 41, pp. 215-229, 2003.

[3] E. G. Njoku, P. Ashcroft and L. Li, “Statistics and global survey of radio frequency interference in AMSR-E land observations,” *IEEE Trans. Geosci. Remote Sensing*, vol. 43, pp. 938-947, 2005.

[4] R.R. Ferraro, “Special sensor microwave imager derived global rainfall estimates for climatological applications,” *J. Geophys.Res.*, vol. 102, pp. 16715-16735, 1997.

[5] J.R. McCollum and R.R. Ferraro, “Next generation of NOAA/NESDIS TMI, SSM/I, and AMSR-E microwave land rainfall algorithms,” *J. Geophys. Res.*, vol. 108, 10.1029/2001JD001512, 2003.

[6] Adler, R., T. Wilheit, Jr., C. Kummerow, and R. Ferraro. 2004, updated daily. *AMSR-E/Aqua L2B Global Swath Rain Rate/Type GSFC Profiling Algorithm V001*, March to June 2004. Boulder, CO, USA: National Snow and Ice Data Center. Digital media.

[7] P. Ashcroft and F. Wentz, “Algorithm theoretical basis document, AMSR level 2A algorithm,” *RSS Tech. Report 121 599B-1*. Santa Rosa, CA: Remote Sensing Systems, 2000.

[8] Njoku, E. 2004, updated daily. *AMSR-E/Aqua L2B surface soil moisture, ancillary parms, & QC EASE-Grids*, March to June 2004. Boulder, CO, USA: National Snow and Ice Data Center. Digital media.

[9] R.R. Ferraro, E.A. Smith, W. Berg, G.J. Huffman, “A Screening Methodology for Passive Microwave Precipiatation Retrieval Algorithms,” *Journal of the Atmospheric Sciences.*, vol. 55, pp. 1583-1560, 1998